Journal of the European Ceramic Society 20 (2000) 1883–1894

Retention of SiC during development of SiC-$M_xSi_yO_z$ composites [M = Al, Zr, Mg] by reaction bonding in air

A.K. Samanta, K.K. Dhargupta, S. Ghatak *

Central Glass & Ceramic Research Institute, Calcutta, India

Received 14 September 1999; received in revised form 7 March 2000; accepted 15 March 2000

Abstract

Oxidation of SiC is a major constraint during development of metal oxide–silicon carbide composites when processed in oxygen containing environment such as in air. In the present investigation, Mg^{+2}, Al^{+3} and Zr^{+4} hydrogels were used as a source of respective oxide and oxidation of SiC in each system was studied. A three-stage mechanism was found to be operative in Al^{+3} and Zr^{+4} systems where oxidation at the initial stages was found to be controlled by the nature of the polynuclear complexes formed on the surfaces of SiC particles. At the intermediate stage a transition from polynuclear complex to metal silicate protective layer formation changes the oxidation characteristics. Finally the metal silicates provided the ultimate protection. Mg^{+2} was found to be ineffective. The extent of retention of SiC in the final composites could be premonitored by controlling the amount and the nature of complexing cations.

Keywords: Composites; Oxidation; Reaction bonding; SiC; Silicates

1. Introduction

Silicon carbide is established to be a good compositing material when dispersed in different oxide matrix[1–7] for improving mechanical[8–10] and other[11] properties of the sintered products. But SiC is prone to oxidation[12] which necessitates an inert atmosphere for sintering[13]. Hot pressing under an inert environment[14,15] is a frequently used mean of forming sintered products. Recently developed reaction bonding techniques[16–19] yielded commendable results but the processes are not likely to be economically viable due to the use of costly raw materials like metals and most importantly due to the conversion of a major amount of SiC into SiO_2. In the processes where metals were either converted to oxides[20] or directly metal oxides[21] were used, the reaction between SiO_2 and the metal oxide starts at a high temperature (~1200°C) with excessive oxidation of SiC. It is possible to provide a protective device to retain SiC at the initial stages by forming a gel-like layer on SiC particles and reaction temperature could be reduced by in situ generation of highly reactive reactants so that a protective layer is formed even before the collapse of the gel structure[22,23] occurs.

In the present work, a systematic study is conducted to formulate a suitable system to retain the maximum possible amount of SiC in the compacts consisting of oxides and silicates of Al, Zr or Mg with an ultimate objective of developing fully dense bodies containing SiC as one of the principal components in a predetermined amount of oxide matrix by forming a gel-like metal polynuclear complex on the surfaces of SiC particles followed by heat treatment at sintering temperature.

2. Experimental[1]

Fine powder of SiC[2] (SiC — 98.8%, C — 0.5%, Si — 0.15%, Al_2O_3 — 0.07%, Fe_2O_3 — 0.08%) was thoroughly dispersed in a requisite amount of 0.5 molar $Mg(NO_3)_2$ $6H_2O$, $Al(NO_3)_3$ $9H_2O$ and $ZrOCl_2$ $8H_2O$ (E.Merck) solution for preparing a respective SiC–metal oxide

[1] The preparation part is applied for protection in India by patent application No. 376/DEL/98.

[2] Carborundum Universal, India.

* Corresponding author.

0955-2219/00/$ - see front matter
PII: S0955-2219(00)00082-0

composite precursor. To this stirred solution 1:1(v/v) liquid ammonia was slowly added. The viscosity gradually increased and ultimately led to complete gelation. The pH of the hydroxide precipitation was adjusted according to the requirement for complete precipitation of the specific cations as hydroxide. The extraneous soluble impurities were removed by washing with water and the precipitate was dried at (50±5°C). The characteristics of the powder precursors of hydroxide hydrogels both with or without SiC were examined by surface area measurement[3] (Table 1), DTA and TGA[4]. The powder was then further heat treated at 800°C for 2 h, milled and sieved through 100 mesh B.S. Bars and pellets were fabricated from the powder by uniaxial pressing at 25 MPa followed by isostatic pressing at 200 MPa and were subjected to heat treatment in the temperature range of 1000–1400°C with heating rate of 7.5°C/min, cooling rate of 10°C/min and a soaking time of 2 h in ambient gas atmosphere. Since in this system increase in weight of the specimens were due only to the oxidation of SiC, it was measured gravimetrically and calculated on the basis of SiC present in the specimens. Identification of different crystallographic phases generated due to heat treatment was studied by XRD[5]. IR spectroscopy[6] on green powder as well as on fired specimens was done.

3. Results

3.1. DTA and TGA of different specimens

For the Al^{+3}-SiC system major weight loss was below 200°C and complete dehydration was noted above 500°C (Fig. 1). A slight weight gain above 850°C was due to the oxidation of SiC. DTA peak at 271.9°C was due to the dissociation of ammonium nitrate formed during processing. For Zr^{+4}–SiC system major weight loss was noted below 200°C and complete dehydration was around 450°C (Fig. 2). In Mg^{+2}–SiC system weight loss was sharp at around 450°C and specimens were completely dehydrated at that temperature (Fig. 3). In this system oxidation of SiC was initiated above 800°C and was substantial at 1200°C up to which the experiment was performed.

No compound formation for Al_2O_3 was noticed in the Al^{+3}–SiC system. In the Zr^{+4}–SiC system a definite and sharp change at 486°C was observed and in the Mg^{+2}–SiC system a sharp peak was recorded above 1100°C.

Table 1
Batch composition and surface area for different systems

System	Batch No	SiC wt%	Al_2O_3 wt%	ZrO_2 wt%	MgO wt%	Sp. surface area (m^2/gm)
SiC–Al_2O_3	A-1	90	10	–	–	88.35
	A-2	80	20	–	–	93.45
	A-3	70	30	–	–	98.34
	A-4	60	40	–	–	102.45
	A-5	50	50	–	–	106.78
	A-6	40	60	–	–	110.00
SiC–ZrO_2	Z-1	90	–	10	–	63.78
	Z-2	80	–	20	–	68.32
	Z-3	70	–	30	–	77.43
	Z-4	60	–	40	–	88.02
	Z-5	50	–	50	–	94.78
	Z-6	40	–	60	–	95.32
SiC–MgO	M-1	90	–	–	10	56.78
	M-2	80	–	–	20	66.98
	M-3	70	–	–	30	72.67
	M-4	60	–	–	40	83.56
	N-5	50	–	–	50	87.34
	M-6	40	–	–	60	93.09

3.2. IR studies

IR spectroscopy of the specimens dried at 110°C and heat treated at 1200°C for 2 h for three different systems is shown in Figs. 4–6.

IR absorption band at 3170 and 1382 cm^{-1} was for NH_4^+ for which a DTA peak was also observed at 271.9°C. O–H stretching vibration at 3460 cm^{-1}, H–O–H vibration at 1757 cm^{-1} and Al–O bonds at 1068 and 627 cm^{-1} were noted for specimens which were not heat treated. On heat treatment at 1200°C absorption bands for NH_4^+ were completely eliminated and peak intensities for other types of bonding were found to be substantially reduced. For Zr^{+4} containing specimens similar observations as was observed for the Al^{+3}–SiC system characterised the system. But the OH stretching vibration at 3387 cm^{-1} almost disappeared when Zr^{+4}–SiC material was heat treated at 1200°C leaving a very weak absorption band at 3470 cm^{-1}. In the Mg^{+2}–SiC system a sharp peak was observed at 3700 cm^{-1} which was due to the O–H-bonds in Mg^{+2} system which was followed by another peak at 3446 cm^{-1} due to O–H stretching vibration. The peak due to O–H bonding disappeared completely when the specimen was heat treated at 1200°C. At this heat treatment temperature SiC oxidised to SiO_2 which was also reflected by the presence of Si–O bonding vibrations at 900 and 962 cm^{-1}.

3.3. Oxidation studies

The initial raw materials were taken in such a proportion that would yield a composition of the samples as shown in Table 1. After processing, the final

[3] Micromentics 220/00000/00, USA.
[4] Model No. STA -409C, NETZSCH.
[5] PW-1730 X-ray Crystallographic Unit provided with a proportional counter PW-1050/70 Goniometer, Philips.
[6] Perkin-Elmer, Model No. -1615, FTIR Spectrometer.

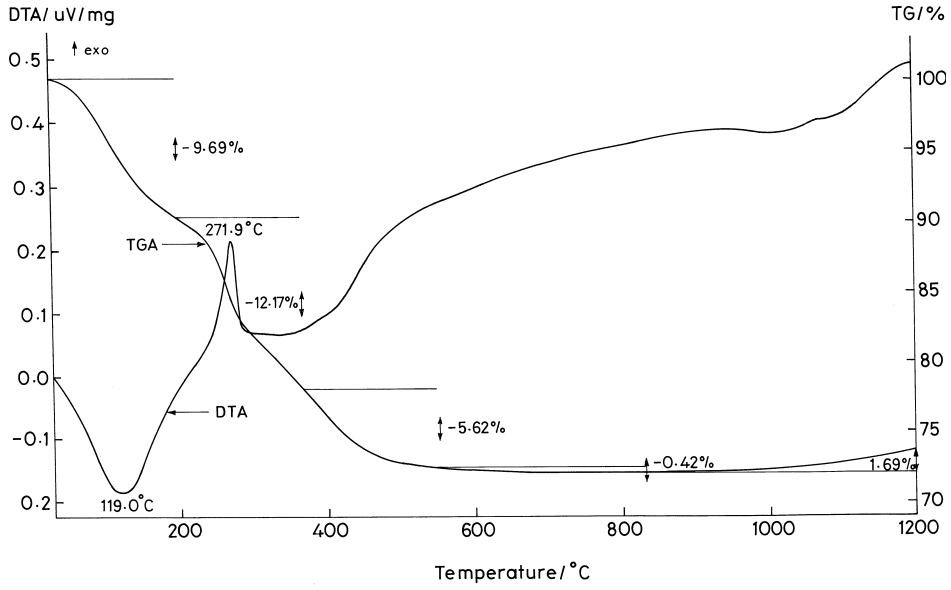

Fig. 1. DTA and TGA curves of the SiC–Al_2O_3 system (50/50 wt/wt).

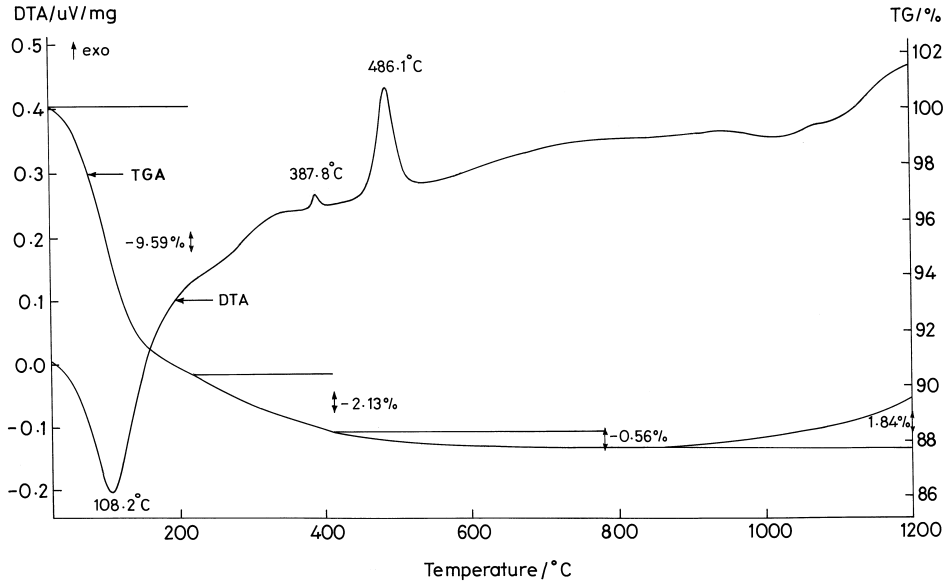

Fig. 2. DTA and TGA curves of the SiC–ZrO_2 system (50/50 wt/wt).

powdered samples had a surface area of 55–110 m^2/gm. Thermogravimetry of the pure gel prepared for comparison indicated water content of 49.59, 25.45 and 32.19% for Al^{+3}, Zr^{+4} and Mg^{+2} systems respectively. For cations Al^{+3} and Zr^{+4}, maximum water was lost at 150–200°C followed by a loss at 450–480°C. However, almost complete dehydroxylation of gel water occurred only above 800°C as was observed by thermogravimetry (Figs. 1 and 2).

Oxidation of SiC was found to initiate above 800°C in agreement to the earlier observation.[21] Oxidation progressed slowly upto 1100°C for specimens containing Al_2O_3 (Fig. 7). The extent of oxidation was lower for specimens containing higher amount of Al_2O_3. Beyond 1100°C extent of oxidation was more and a saturation value for oxidation was reached at around 1300°C for all specimens. Here again, extent of oxidation of SiC was found to be strongly dependent on the amount of the Al_2O_3 present in the specimens. Higher the Al_2O_3 content lower was the extent of oxidation of SiC. The discontinuous line shown in Fig. 7 indicated the extent of oxidation of SiC where Al_2O_3 was absent. Though an almost complete protection of SiC was observed for all the specimens containing Al_2O_3, for the specimen containing no Al_2O_3 a rising trend was noted under the same conditions.

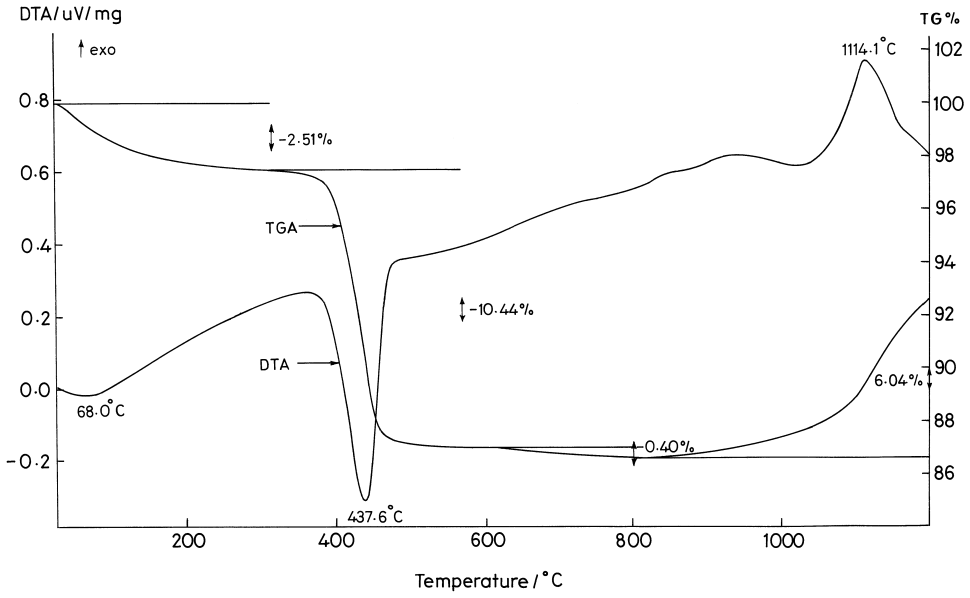

Fig. 3. DTA and TGA curves of the SiC–MgO system (50/50 wt/wt).

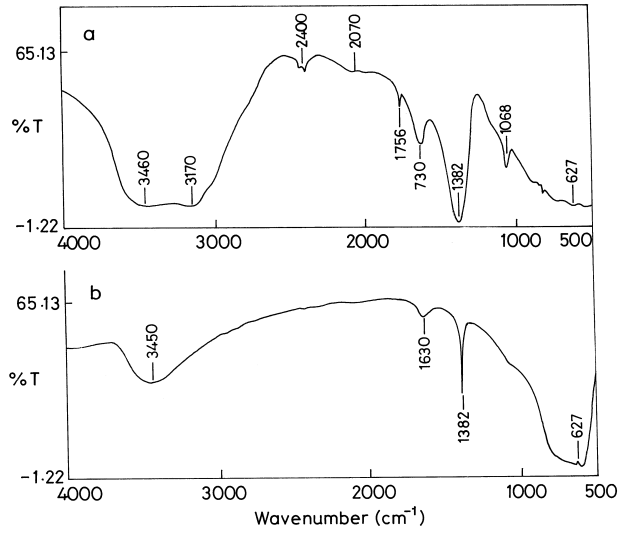

Fig. 4. IR Spectroscopy of the Al_2O_3 gel–SiC mixture (50/50 wt/wt) (a) Heat treated at (110°C), (b) Heat treated at (1200°C).

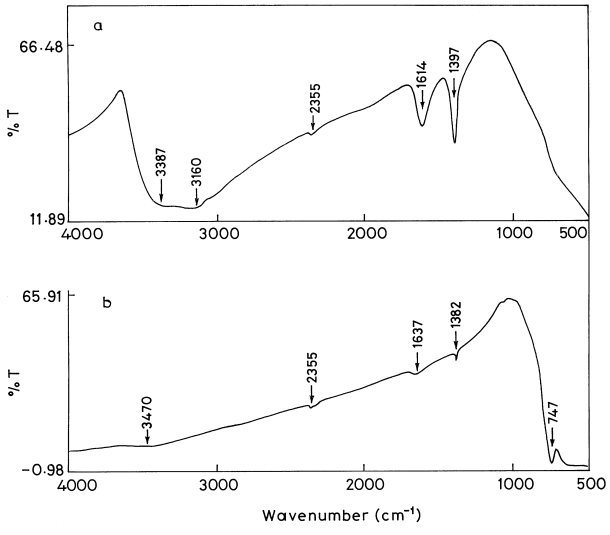

Fig. 5. IR Spectroscopy ZrO_2 gel–SiC mixture (50/50 wt/wt). (a) Heat treated at (110°C), (b) Heat treated at (1200°C).

When similar experiments were conducted with Zr^{+4} system oxidation of SiC was found to be more (Fig. 8), almost double, in the temperature range of 1000–1100°C in comparison to that of Al^{+3} system (Fig. 7). With the increase in temperature of heat treatment, oxidation of SiC in Zr^{+4} system decreased but the limiting value could not be reached. If compared with Al^{+3} system, Zr^{+4} provided less protection to oxidation of SiC. In presence of Mg^{+2}, oxidation of SiC linearly increased with the increase in temperature of heat treatment as well as with the increase in amount of Mg^{+2} (Fig. 9). Thus, it may be said that Mg^{+2} in the system accelerated the process of oxidation of SiC.

Therefore, the conclusion that can be drawn at this stage is that, in the present systems, oxidation of SiC was best prevented by Al^{+3} followed by Zr^{+4}. Mg^{+2} accelerated the process of oxidation of SiC instead of preventing it.

3.4. XRD analysis

XRD patterns of the specimens for three systems are shown in Figs. 10–12. All specimens were fired at 1400°C in ambient atmosphere with 2 h soaking. Mullite and SiC were found to be the major phases along with trace amount of Al_2O_3 in Al^{+3}–SiC system. It was

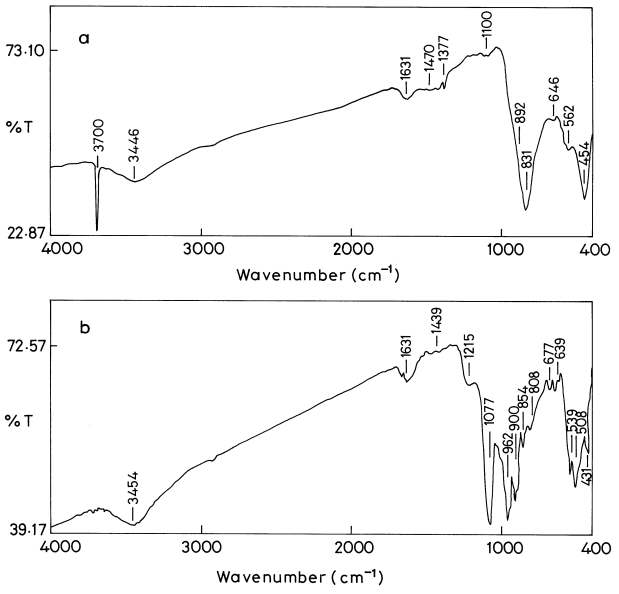

Fig. 6. IR Spectroscopy MgO gel–SiC mixture (50/50 wt/wt). (a) Heat treated at (110°C), (b) Heat treated at (1200°C).

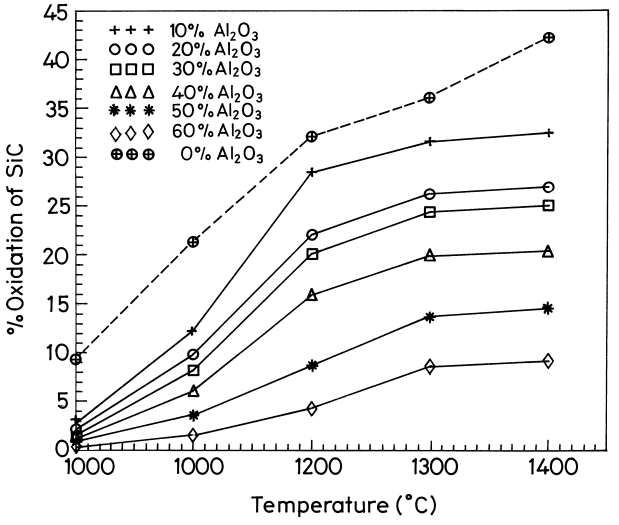

Fig. 7. Oxidation of SiC at different temperature in the SiC–Al_2O_3 system.

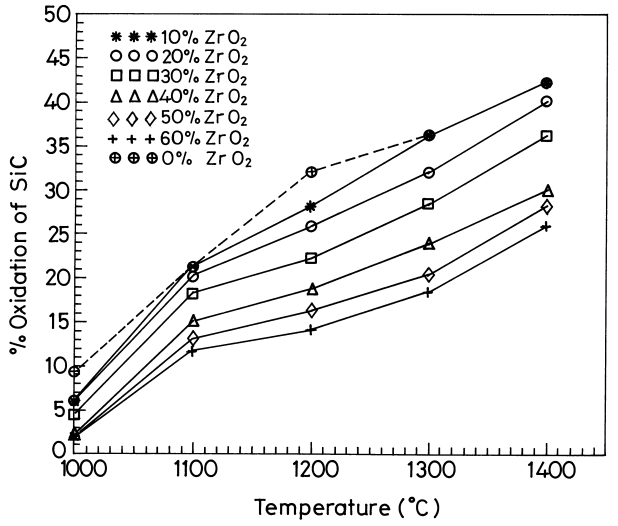

Fig. 8. Oxidation of SiC at different temperature in the SiC–ZrO_2 system.

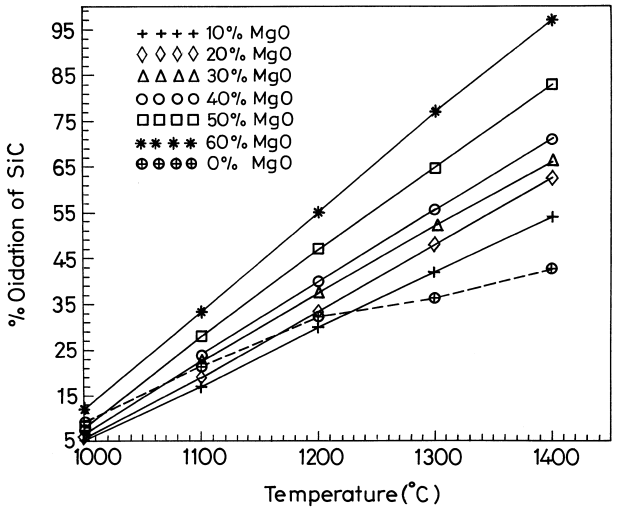

Fig. 9. Oxidation of SiC at different temperature in the SiC–MgO system.

4. Discussion

4.1. Nature of protective coating (up to 1100°C)

In the sample preparation stage, SiC was brought into suspension in moderately high solid loading and high electrolytic concentration. It is expected that Mg^{+2}, Al^{+3} and Zr^{+4} in aqueous dispersions will establish an ionic equilibrium with negatively charged SiC particles. With increase in concentration of higher valent cations, charge reversal takes place due to excess cationic adsorption. This was supported by rheological analysis of this type of system.[24] The increase of viscosity[25] of such a system lent credence to the assumption that by particle association the floc structure was formed. As an elaboration it may be said that in a polydispersed sys-

evident from the peak intensities that the amount of mullite increased with the increase in amount of Al_2O_3. At lower Al_2O_3 containing specimens ($\leqslant$30 wt%) cristobalite was detected along with mullite and SiC (Fig. 13). In Zr^{+4}–SiC system $ZrSiO_4$ and SiC were detected as the major phases and cristobalite as minor phase. The cristobalite was still present at higher ZrO_2 containing specimens but the amount decreased with the increase in amount of ZrO_2 (Fig. 11). In Mg^{+2}–SiC system, cristobalite and $MgSiO_3$ (enastatite) were found as the major phases and the amount of both increased with the increase in amount of MgO (Fig. 12).

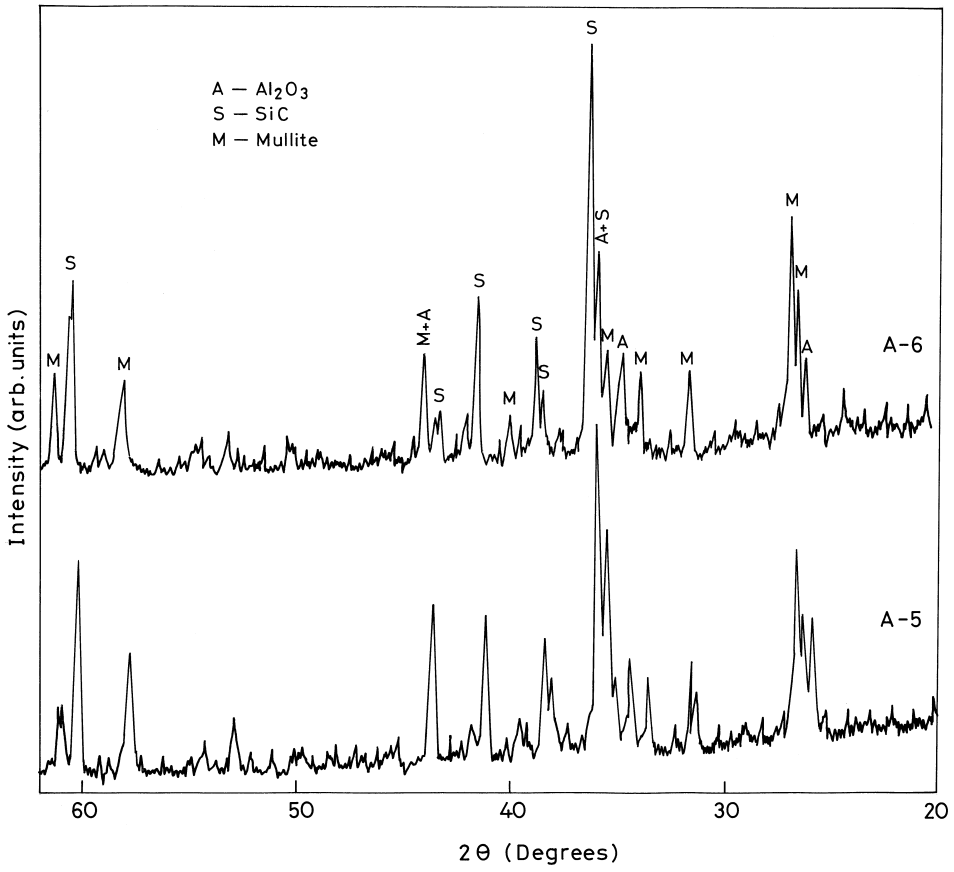

Fig. 10. XRD analysis of fired specimens (1400°C) in the SiC–Al_2O_3 system containing Al_2O_3 > 30 wt%.

tem, like the present one (Fig. 14), voids between large particles were filled in by smaller particles leading to negligible liquid trapping. Again, slurry of high solid content as in the present system may be assumed to be in a state of "aggregated liquid holding floc".[26,27] In the presence of cations in highly concentrated state in the slurry of SiC, the formed flocs were likely to consist of particles held together by a combination of colombic and Vander waal's forces for forming a network. This network was in pseudo-equilibrium state which was readily converted to a polymeric network by OH^- bridging in the presence of hydroxide. SiC particles, already coated by metal cations by colombic forces of attraction remained fixed in the hydrogel network forming a gel-like semisolid mass due to ion-dipole interaction in the anionic framework.[28] The entire phenomenon may be explained as follows:Al^{+3} forms complexes $[Al(OH_2)_6]^{+3}$, water of which was gradually replaced by OH^- ions during reaction with hydroxide more or less in the following sequence: $[Al\,(OH_2)_6]^{+3} \rightarrow [Al(OH)\,(OH_2)_5]^{+2} \rightarrow [Al(OH)_2\,(OH_2)_4]^{+1} \rightarrow [Al\,(OH)_3\,(OH_2)_3]^0$ Polymerisation proceeded with the formation of polynuclear complexes[29,30] as shown in Fig. 15.

The Zr^{+4} atoms have a co-ordination number of 8 and are connected through OH bridges. Each Zr^{+4} atom is surrounded by four water molecules. The oxygen atoms of the water and of the OH groups are located at the apexes of the square antiprism[30,31] as shown in Fig. 16.

Nature of the polynuclear complexes depended on the number and type of the metal cations and their ability to form a network structure. The amounts of Al^{+3} in a system were found to have a great influence on the oxidation characteristics of SiC particles. The same observation was found to be true in the Zr^{+4} system also. With an increasing number of Al^{+3} and Zr^{+4}, oxidation tendency of embedded or "caged" SiC particles diminished.

In the Al^{+3} system, the number of OH bridges was more than that of Zr^{+4} system (Figs. 15 and 16) and it may be one of the major factors for more protection of SiC grains in 1000–1100°C range in this system. If this presumption is true then the Mg^{+2} system was not expected to provide any protection to oxidation of SiC particles as above 500°C Mg $(OH)_2$ lost all water without leaving any OH bridge in the system as anionic complexes were not characteristics of Mg^{+2}. This explains the present observation when it was found that oxidation of SiC in the Mg^{+2} system increased linearly with increasing heat treatment irrespective of compositions. Further confirmation of the role of OH-bridging

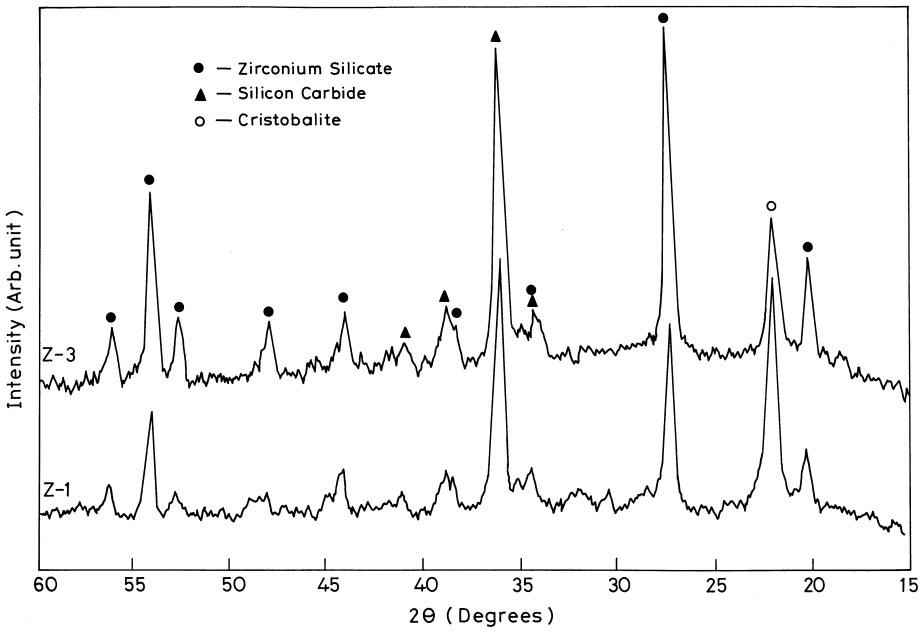

Fig. 11. XRD analysis of fired specimens (1400°C) in the SiC–ZrO_2 system.

in oxidation prevention were obtained by IR measurements of heat treated samples which indicated the existence and gradual removal of OH during heat treatment of the specimens (Fig. 6).

4.2. Oxidation of SiC

On progressive heat treatment, water was detached from the structure. Al–OH bonding is stronger than Zr–OH bonding due to lower ionic radius of Al^{+3} (0.057 nm) than that of Zr^{+4} (0.082 nm). Consequently protection of SiC in the initial stages (1000–1100°C) was more in the Al^{+3} system than that in the Zr^{+4} system.

In the temperature range of 1100–1400°C two mechanisms were likely to operate simultaneously viz. (a) collapse of gel structure with the elimination of OH-bridges generating cracks and holes, facilitating oxygen transportation to the SiC surface resulting into higher oxidation and (b) formation of silicates by combination of the oxidation product of SiC i.e. SiO_2 and metal oxides formed from hydrogel resulting in a protective silicate coating on SiC surfaces. The role of different matrix materials that surrounded individual SiC particles towards building up of resistance for SiC oxidation might be analysed on the basis of oxygen diffusivity. As had been discussed elaborately[32] for the oxidation of an "individual" SiC particle in a metal oxides matrix, oxygen first diffused through the metal oxide matrix to the surface of SiC which was already coated with SiO_2. Therefore, oxidation of SiC particles depended on the diffusivities of oxygen through (i) the metal oxide matrix and (ii) the SiO_2 on the surface of SiC at the initial stage. At the later stages, oxidation of SiC particles would depend on the diffusivities of oxygen through (i) the metal oxide matrix and (ii) metal silicates formed on the surface of SiC assuming that all the SiO_2 on the SiC surface was converted to metal silicates that remained on the SiC surface as a coating.

4.2.1. Al^{+3}–SiC

It appeared from Fig. 7 that oxidation of SiC in the Al^{+3} system (measured gravimetrically from the weight gain of SiC and calculated on the basis of the weight of SiC) was faster in the range 1100–1200°C than the preceding range. As silica was formed at the surface of SiC particles during oxidation, it might be assumed that the surface of SiC particles became silica rich. Here the reaction between SiO_2 and Al_2O_3 proceeded in the following sequence: (i) Al_2O_3 dissolved in amorphous SiO_2 matrix, (ii) mullite nuclei formed within this matrix as the matrix composition exceeded the saturation limit with respect to mullite and (iii) mullite crystals grew as more Al_2O_3 dissolved into the matrix and then was incorporated into the growing mullite grains. The above sequence was proposed[33,34] on the observation that in the temperature range <1500°C, mullite formed by a nucleation and growth process within the silica-rich matrix and not at the alumina interfaces, as the siliceous matrix was saturated with respect to mullite through the dissolution of alumina. So, it was expected that as the reaction proceeded, SiC particles would be progressively coated by mullite, gradually blocking the path of oxygen, thus preventing further oxidation. Extent of oxidation decreased markedly on increasing the aluminium component and with 60 wt% Al_2O_3 in the system, oxidation reduced to less than 10% at 1400°C whereas the

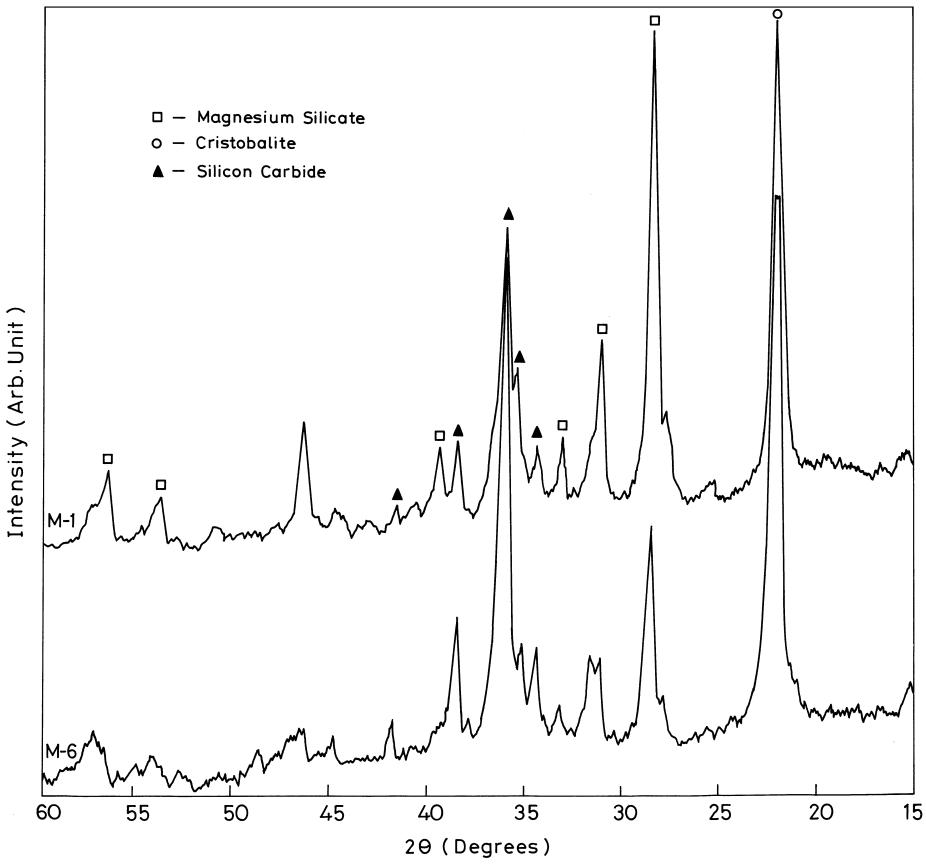

Fig. 12. XRD analysis of fired specimens (1400°C) in the SiC–MgO system.

oxidation was more than 30% when Al_2O_3 used in the system was 10%.

XRD analysis of specimens containing different amounts of Al_2O_3 fired at different temperatures (Fig. 13) indicated the presence of cristobalite, mullite and SiC. The cristobalite phase decreased with increasing amount of Al_2O_3 and the samples containing >30 wt% Al_2O_3, fired at 1400°C were found to contain Al_2O_3, SiC & mullite only (Fig. 10).

4.2.2. Zr^{+4}–SiC

Unlike the Al^{+3} system, polynuclear hydrogel structure formed by Zr^{+4} is less stable as had already been discussed in Section 4.1. But the most striking difference between the Al^{+3} system and Zr^{+4} systems was the characteristic of oxidation at temperature above 1100°C. For the Al^{+3} system, oxidation increased more rapidly when specimens were fired above 1100°C, but in the Zr^{+4} system it was less. Formation of $ZrSiO_4$ by the reaction[35] of ZrO_2 and SiO_2 (formed by oxidation of SiC) offered better oxidation protection in the temperature range 1100–1400°C. Like the Al^{+3} system, here also, further oxidation of SiC particles was protected and was strongly dependent on Zr^{+4} concentration. This was so because $ZrSiO_4$ in the present system started forming as soon as SiO_2 was made available to the system by the oxidation of SiC. In the temperature range of 1000–1100°C, moderately higher oxidation of SiC generated quite a large amount of silica thus facilitating the formation of more $ZrSiO_4$ which explained the marked increase of oxidation protection with increasing ZrO_2 in the specimens.

Depending on crystal structure, additives, and stoichiometry, oxygen diffusivity in ZrO_2 is between 10^{-9}–10^{-5} $cm^2\ s^{-1}$ at 1000°C.[36,37] At the same temperature, oxygen diffusivity in amorphous silica is 10^{-13}–10^{-12} $cm^2\ s^{-1}$.[38,39] Diffusivity in mullite is 10^{-20}–10^{-18} $cm^2\ s^{-1}$ [40,41] which was assumed to be similar to that of in Al_2O_3. Therefore, formation of ZrO_2 by dehydration and dehydroxylation of the polynuclear hydrogel structure was expected to increase oxidation of SiC at lower temperature range. But, the combination of ZrO_2 with SiO_2 at higher temperature leading to the formation of $ZrSiO_4$ substantially reduced ZrO_2, thus decreasing oxygen transport as well as providing $ZrSiO_4$ phase in which oxygen diffusivity was suggested[32] to be substantially low as in the case of silicon oxynitride-zirconia composites.[42] When oxides were used, $ZrSiO_4$ formed at 1200°C but when hydrogel was used as a source of ZrO_2, $ZrSiO_4$ formed at around 1000°C

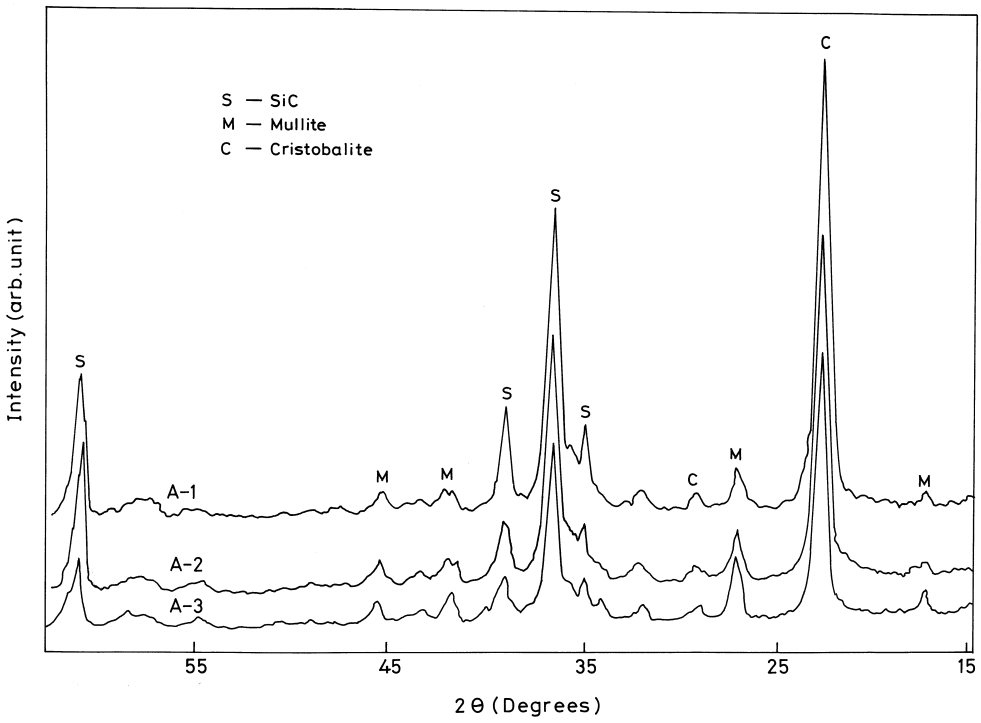

Fig. 13. XRD analysis of fired specimens (1200°C) in the SiC–Al_2O_3 system containing Al_2O_3 ⩽30 wt%.

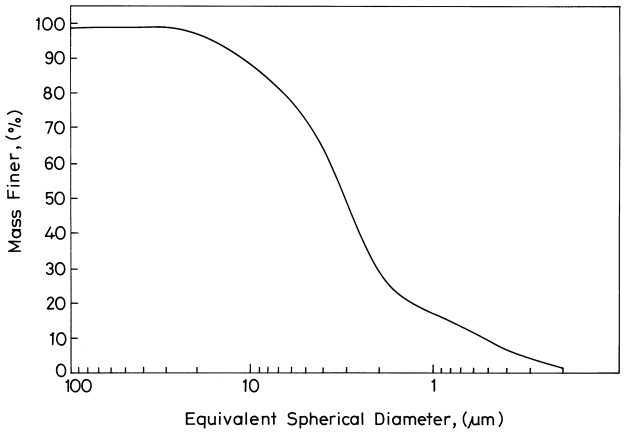

Fig. 14. Particle size distribution of SiC powder.

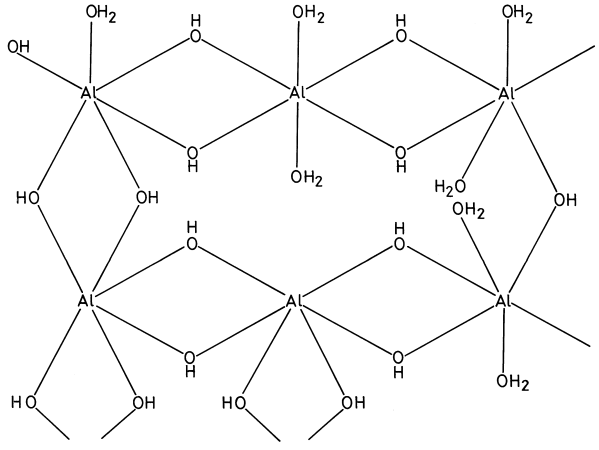

Fig. 15. Polynuclear complex in the Al–OH–H_2O system.

(observed by XRD analysis). ZrO_2:SiO_2 molar ratios were calculated on the basis of oxidation values of SiC for samples fired at different temperatures. The values gave an indication of probable phases, those might form at different temperatures of heat treatment. ZrO_2–SiO_2 phase diagram suggested the formation of $ZrSiO_4$ with SiO_2 as tridymite or cristobalite in this temperature range. For a sample containing ZrO_2 in the range upto 40 wt%, ZrO_2:SiO_2 molar ratio was always <1 indicating SiO_2 rich phases at all temperature. Specimens might be divided into two groups with some approximation. One group of samples containing upto 40 wt% ZrO_2, should contain excess silica in addition to $ZrSiO_4$ after heat treatment upto 1400°C as the molar ratio of ZrO_2:SiO_2 fell below 1. But the other group of samples, containing above 40wt% ZrO_2, mostly $ZrSiO_4$ was expected as the molar ratio of ZrO_2:SiO_2 was >1. The rapid oxidation of SiC occurred upto 1200°C instead of 1100°C which was noted for the first group.

4.3. Relative influences of Al^{+3}, Zr^{+4} and Mg^{+2} on oxidation of SiC

Keeping all parameters identical, samples were prepared with 35 wt% of MgO, Al_2O_3 and ZrO_2 (derived through respective hydrogels) and 65 wt% SiC in aqueous medium. Percent oxidation in these systems was measured after firing the specimens at 1300°C with 2 h

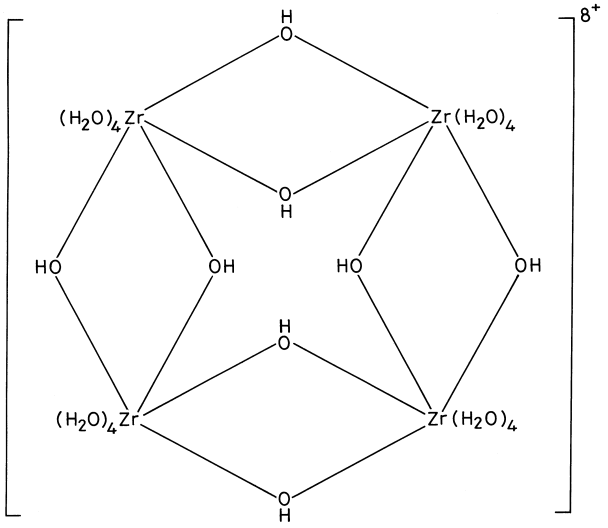

Fig. 16. Polynuclear complex in the Zr–OH–H_2O system.

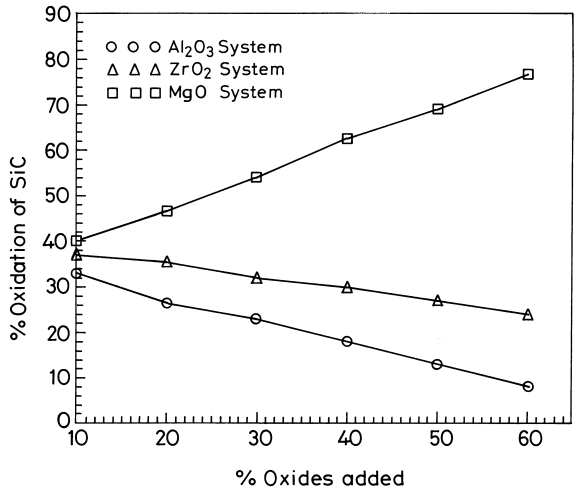

Fig. 17. Comparision of extent of oxidation of SiC in presence of Al^{+3}, Zr^{+4} and Mg^{+2} fired at 1300°C with 2 h soaking.

soaking and shown in Fig. 17. The figure depicted a qualitative view of relative action of three oxides in providing oxidation protection to SiC particles. Al_2O_3 was found to be best followed by ZrO_2. MgO was found to provide no protection at all. This behaviour of Mg^{+2} is in conformity with the observation that most trivalent and qurdrivalent ions form polynuclear species whereas the process only occurs with the smallest of the divalent ions-Be^{+2} (0.034 nm) and not with Mg^{+2} (0.068 nm).

For both Al^{+3} and Zr^{+4} systems fast oxidation of SiC occurred upto 30 wt% oxide content. The initial fast oxidation stage is extended up to 50 wt% of Al_2O_3 and 60 wt% of ZrO_2 content. For samples containing 60 wt% Al_2O_3, the initial oxidation stage continued upto 1300°C. The extension of temperature range for initial oxidation stage, in effect, helped in better protection of SiC grains as it gave extended scope for the reaction $2\ SiO_2 + 3\ Al_2O_3 = 3\ Al_2O_3.2SiO_2$ and $SiO_2 + ZrO_2 = ZrSiO_4$ to occur and form a second protective coating on the SiC surfaces before the first gel-coating goes off completely. So, at this stage a general mechanism may be put forward for the entire phenomenon as shown in Fig. 18. Mg^{+2} was not likely to form polynuclear complex in the aqueous system and was completely dehydrated at 500°C. So, Mg^{+2} will not participate in the above mechanism. Being basic in character, MgO combined with SiO_2 forming magnesium silicate. Oxidation of SiC increased remarkably when Mg^{+2} is incorporated in the system as compared with other two systems of Al^{+3} and Zr^{+4} (Fig. 17). The role of Mg^{+2} was found to be just opposite to that of Al^{+3} and Zr^{+4}. Instead of protecting SiC grains, Mg^{+2} was found to accelerate the oxidation of SiC grains by continuously removing the natural protective SiO_2 layer on SiC thus continuously creating fresh surfaces for attack by oxygen. The fired compacts were found to have meso-enastatite, cristobalite with silicon carbide (Fig. 12).

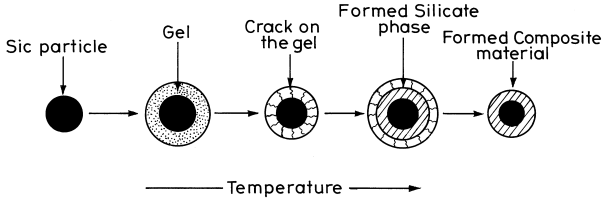

Fig. 18. Schematic model flow-diagram of the process mechanism.

5. Conclusion

(1) SiC particles being negatively charged in aqueous suspension adsorbed metal cations on its surface by coulombic and van der Waal's forces. Those metal cations are converted to polynuclear metal hydroxy complexes in presence of hydroxyl ion in the system. As a result a gel-like mass was formed in which individual SiC particles remained more or less uniformly distributed.

(2) On dehydration, the gel-like mass formed a layer on the SiC particles and provided a protection to oxidation of SiC by creating different types of barriers for oxygen transportation from environment to the SiC-surface up to 1200°C. The effectiveness of such a second material towards blocking the path of oxygen depended on the nature of the cations that formed polynuclear complexes.

(3) The cations that were capable of forming larger network were found to be capable of providing better protection towards oxidation of SiC.

(4) At higher temperature (>1200°C), the gel structure collapsed leaving cracks and exposing more surface of SiC particles towards oxidation and at this stage protection to the SiC grains were provided by the silicates formed from SiO_2 (formed by the oxidation of SiC) and metal oxide (formed by dehydration and dehydroxylation of gel).

(5) At the initial stage, Al^{+3} -system provided better protection as it formed more stable gel structure than Zr^{+4} -system. But as the temperature increases Zr^{+4} system gave better protection to oxidation of SiC because formation temperature of oxidation protective Zr-silicate was lower than that of Al-silicate. The delayed initiation of the reaction bonding in Al^{+3}-system, however, was adequately compensated by the efficient protection of SiC grains at the initial stage.

(6) The overall protective effect was better in Al^{+3} - system than that in Zr^{+4} - system. Mg^{+2} - system did not provide any protection as Mg^{+2} was neither capable of forming extended polynuclear hydroxy complex nor it could provide any protective reaction products. The enastatite formed continuously removed SiO_2 from SiC surfaces thus indirectly catalysing the process of oxidation of SiC.

Acknowledgements

Authors are deeply indebted to Prof. N. K. Mitra, Dept. of Chem. Tech., University of Calcutta for his valuable suggestions and active help during preparation of the manuscript. Thanks are also due to Dr. B. Karmakar for doing IR spectroscopy, to Mr. B. P. Ghosh for thermal analysis and various other departments providing infra-facilities. Authors are grateful to Director CG & CRI, for his personal interest in this work.

References

1. Kim, S. and Kriven, M. W., Preparation, microstructure, and mechanical properties of silicon carbide–dysprosia composites. *J. Am. Ceram. Soc.*, 1997, **80**(12), 2997–3008.
2. Belmonte, M. and Miranzo, P., Al_2O_3/SiC platelet composites : Effect of sintering conditions. *J. Eur. Ceram. Soc.*, 1997, **17**, 1253–1258.
3. Miao, X., Rainforth, W. M. and Lee, W. E., Dense zirconia–SiC platelet composites made by pressureless sintering and hot pressing. *J. Eur. Ceram. Soc.*, 1997, **17**, 913–920.
4. Yang, X. and Rahaman, M. N., SiC platelet - reinforced Al_2O_3 composites by free sintering of coated inclusions. *J. Eur. Ceram. Soc.*, 1996, **16**, 1213–1220.
5. Deng, Y. Z., Zhang, F. Y., Shi, L. J. and Guo, K. J., Microstructure and flexure creep behaviour of SiC - particle reinforced Al_2O_3 matrix composites. *J. Eur. Ceram. Soc.*, 1996, **16**, 1337–1343.
6. Chou, Y. S. and Green, D. J., Processing and mechanical properties of a silicon carbide platelet/alumina matrix composite. *J. Eur. Ceram. Soc.*, 1994, **14**, 303–311.
7. Lin, T. H., Alexander, K. B. and Becher, P. F., Grain size effect on creep deformation of alumina–silicon carbide composites. *J. Am. Ceram. Soc.*, 1996, **79**(6), 1530–1536.
8. Moffatt, J. E., Plumbridge, W. J. and Hermann, R., High temperature crack annealing effects on fracture toughness of alumina and alumina - SiC composite, *Brits. Ceram. Trans.*, 1996, **95**(1), 23–29.
9. Thompson, A. M., Helen, M. C., Harmer, M. P. and Cook, R. F., Crack healing and stress relaxation in Al_2O_3–SiC "nanocomposites". *J. Am. Ceram. Soc.*, 1995, **78**(3), 567–571.
10. Levin, I., Kaplan, W. D., Brandon, G. and Layyous, A. A., Effect of SiC submicrometer particle size and content on fracture toughness of alimina–SiC "Nanocomposites". *J. Am. Ceram. Soc.*, 1995, **78**(1), 254–256.
11. Murthy, V. S. R. and Deepak, A., Microstructure and mechanical properties of SiC–Al–Al_2O_3 composites prepared by direct melt infiltration. *Brits. Ceram. Trans.*, 1996, **95**(4), 173–176.
12. Wu, S. and Claussen, N., Fabrication and properties of low-shrinkage reaction bonded mullite. *J. Am. Ceram. Soc.*, 1991, **74**(63), 2460–2463.
13. Alliegero, R. A., Coffin, L. B. and Tinklepaugh, J. R., Pressure-sintered silicon carbide. *J. Am. Ceram. Soc.*, 1956, **39**, 386.
14. Yo, Tajima and Kingery, W. D., Grain-boundary segregation in aluminium doped silicon carbide. *J. Mat. Sci.*, 1982, **17**, 2289–2297.
15. Bassett, L. B. and Joseph, A. D., Structure and orientation of hot-pressed silicon carbide- presented at the fifty sixth Annual meeting. The Am. Ceram. Soc., Chicago, III 20 April 1954.
16. Popper, P., *Special Ceramics*, ed.. P. Popper, Heywood Publishing, London, 1960, pp. 209.
17. Popper, P. and Davis, D. G., *Powder Metall*, 1961, **8**, 113.
18. Forrest, C. W., Kennedy, P., and Shennan, J. V., in *Special Ceramics, 5*. Heywood Publishing, London, 1970, pp. 99–123.
19. Taylor, K. M., US Patent No. 3205043, Sept. 7; 1965.
20. Lin, H. T. and Breder, K., Creep deformation in an alumina–silicon carbide composites produced via a direct metal oxidation process. *J. Am. Ceram. Soc.*, 1996, **79**(8), 2218–2220.
21. Wu, S. and Claussen, N., Reaction bonding and mechanical properties of mullite/silicon carbide composites. *J. Am. Ceram. Soc.*, 1994, **77**(11), 2898–2904.
22. Samanta, A. K., Dhargupta, K. K. and Ghatak, S., Prevention of oxidation of SiC through reaction bonding in the SiC–mullite composite systems by using the technique of intermediate gel formation. *Trans, Ind., Ceram., Soc.*, 1998, **57**(4), 103–105.
23. Samanta, A. K., Dhargupta, K. K. and Ghatak, S., Oxidation behaviour of silicon carbide-gel derived oxide composite systems. *Trans, Ind., Ceram., Soc.*, 1998, **57**(5), 119–120.
24. Dhargupta, K. K. and Ghatak, S., Rheological behaviour of silicon carbide suspension in relation to particle size distribution. *Trans, Ind., Ceram., Soc.*, 1993, **52**(5), 167–171.
25. Dhargupta, K. K. and Ghatak, S., Rheological parameters of silicon carbide slips in relation to carbon content and particle size distribution. *Trans, Ind., Ceram., Soc.*, 1993, **52**(6), 215–220.
26. Nagel, A., Petzow, G. and Greil, P., Rheology of aqueous silicon nitride suspensions. *J. Eur. Ceram., Soc.*, 1989, **91**, 371–378.
27. Beazley, K. M., Breakdown and build-up in china clay suspensions. *Trans, Brits., Ceram., Soc.*, 1964, **63**, 451–471.
28. Ghatak, S., Effect of heat treatment on the physico-chemical characteristics of aluminosilicate hydrogel in relation to exchangeable cations. PhD thesis, University of Calcutta, 1977.
29. Akhmetov, N. S. *General and Inorganic Chemistry*, Mir Publishers, Moscow, 1987. pp. 456–457.
30. Cotton, F. A. and Wilkinson, G. *Advanced Inorganic Chemistry: A Comprehensive Text*. Wiley Eastern Private Ltd., 2nd rev., and augmented ed., 1972.
31. Akhmetov, N. S. General and inorganic chemistry. Mir Publishers, Moscow, 1987, p. 536.
32. Tsai, C. Y., Lin, C. C., Zangvil, A. and Li, A. K., Effect of zirconia content on the oxidation behaviour of silicon carbide/zirconia/mullite composites. *J. Am. Ceram. Soc.*, 1998, **81**(9), 2413–2420.
33. Sundarsen, S. and Aksay, I. A., Mullitization of diphasic aluminosilicate gels. *J. Am., Ceram., Soc.*, 1991, **74**(10), 2388–2392.
34. Wei, W. and Hallonan, J. W., Transformation kinetics of diphesic alumino-silicate gels. *J. Am., Ceram., Soc.*, 1988, **71**(7), 581–587.

35. Levin, E. M., Robbins, R. C. and Mc Murdie, H. F., *Phase Diagrams for Ceramists*, 1969 Supplement, Fig. No. - 2400, Edited and Published by The American Ceramic Society, 1993.
36. Kofstad, P., Oxides of group IVA elements. In *Nonstoichiometry, Diffusion and Electrical Conductivity in Binary Metal Oxides*. Robert E. Krieger Publishing, Malabar, FL, 1983, pp. 152–165.
37. Dou, S., Masson, P. R. and Pacey, P. D., Induction period for oxygen permeation through calcia-stabilized zirconia ceramic. *J. Am. Ceram. Soc*., 1989, **72**(7), 1114–1118.
38. Norton, F. J., Permeation of gaseous oxygen through vitreous silica. *Nature (London)*, 1961, **191**, 701.
39. Lamkin, M. A., Riely, F. L. and Fordham, R. J., Oxygen mobility in silicon dioxide and silicate glasses: a review. *J. Eur. Ceram. Soc*., 1992, **10**, 347–367.
40. Luthra, K. L. and Park, H. D., Oxidation of silicon carbide reinforced oxide matrix composites at 1375 to 1575°C. *J. Am. Ceram. Soc*., 1990, **73**(4), 1014,–1023.
41. Cherkasoy, P. A., Ficher, W. A. and Pieper, C., Oxygen permeability of solid electrolytes and its effect on the electrochemical determination of the activity of oxygen in gases and liquid metals (in Ger,). *Arch, Eisenhuettenwes*, 1971, **42**, 873–876.
42. O'Meara, C., Heim, M. and Pompe, R., The oxidation behaviour of a porous Si_2N_2O–ZrO_2 composite material. *J. Eur. Ceram. Soc*., 1995, **15**, 319–328.